Evaluation of the Effects of Distributed Roughness Induced Transition on the EXPERT Vehicle

Guillaume Grossir, Sébastien Paris, Olivier Chazot
von Karman Institute for Fluid Dynamics, Chaussée de Waterloo 72, 1640 Rhode-St-Genèse, Belgium

This work is part of the EXPERT project lead by ESA aiming to study phenomena occurring during Earth reentry for hypersonic vehicles. Transition from laminar to turbulent flows due to distributed roughness on the non-ablative nose of a blunt vehicle can be a big issue for the thermal protection system. Experiments are carried out with different distributed roughness densities, locations and sizes in the Longshot short duration facility (free-stream Mach number of 14, low enthalpy, Reynolds number about 13.10^6/m) at the VKI. Wall temperature measurements with thermocouples on the scaled EXPERT model allow the determination of heat flux and Stanton number. Comparison between experimental and theoretical Stanton numbers allows the detection of transition. Pressure measurements support the transition investigation. Following a complementary approach, empirical correlations (Reda and Reshotko) are evaluated from CFD results to determine the distributed roughness critical height leading to transition. Theory predictions and experimental results are compared to determine how correlations are applicable to the EXPERT geometry. An extrapolation to flight conditions is performed on this basis giving the largest allowable height for distributed roughness.

Nomenclature

$\dot{Q}$	heat flux, W/m^2	t	time, s
ρ	density, kg/m^3	T	temperature, K
Cp	heat capacity at constant pressure	U	velocity, m/s
k	thermal conductivity, W/(m.K)		
M	Mach number		
p	pressure, Pa	Subscripts	
Re	Reynolds number	0	stagnation
St	Stanton number	∞	free-stream
τ	time, s	w	wall

I. Introduction

The surface roughness of a vehicle is a key parameter in the design of a flight vehicle as it may induce early boundary layer laminar-to-turbulent transition. This phenomenon is leading to larger heat transfer at the surface and larger skin friction which can affect the stability of the vehicle and its aerodynamic coefficients.

Nowadays, physics of the boundary layer receptivity and process associated with the growth of disturbances are still poorly understood. Experiments in hypersonic wind-tunnels are needed in order to validate the results obtained from computational fluid dynamics (CFD). These experiments are limited by the requirements of matching flight conditions, both Mach and Reynolds number. Moreover, there is a lack of models able to perform an extrapolation to flight conditions from ground experiments.

The EXPERT project (European eXPErimental Reentry Testbed) has been initiated in 2000 by ESA in order to improve the knowledge of Earth reentries and to validate the development of CFD codes. The EXPERT vehicle has the shape of a blunt cone, its nose is made of a non-ablative ceramic material and the fore-body is smothered by a metallic thermal protection material.

During the orbital re-entry trajectory, the vehicle will experience a maximum heat flux about $1.5.10^6$ W/m^2 which may induce oxidation process on the ceramic material composing the nose of the vehicle. Irregularities resulting from this process are called distributed roughness. The effects of distributed roughness on boundary layer transition on a ground-scaled model of the EXPERT vehicle are described hereafter.

Experiments are performed in the Longshot wind-tunnel at the Von Karman Insitute (VKI). Tests conditions are close to the ones encountered during flight for Mach and Reynolds numbers. Several tests are performed with different sizes of roughness, different densities of roughness, and at different locations. The surface temperature of the model measured by thermocouples allows determining the heat flux to the wall and the Stanton number. Values are compared with results from CFD allowing assessing whether the flow is turbulent or not. Critical heights for the distributed roughness triggering transition in the Longshot facility are determined. Experimental results, giving critical heights, are compared with theoretical heights predicted by two empirical correlations (Reda and Reshotko criteria). These correlations are evaluated through CFD results provided by ESA and matching Longshot test conditions.

The final objective of this research is to conduct an extrapolation to flight conditions and to determine the maximum allowable height resulting from surface oxidation without triggering transition.

II. Experimental Setup

A. Test Facility

All experiments reported have been performed in the VKI Longshot free piston wind-tunnel (Figure 1). This is a low enthalpy short duration facility that can be operated with either nitrogen or carbon dioxide, and it is designed to provide the attainment of very high Reynolds number hypersonic flows. The three main theoretical conditions at which the facility can run are listed in Table **1**. For this study, tests at medium Reynolds number only have been performed as they are the closest ones to the conditions encountered in flight as reported on Figure 2.

The experiments conducted in the frame of this study used a Mach 14 contoured nozzle of 0.43m exit diameter with the use of nitrogen. Instrumentation included coaxial thermocouples for heat flux measurements, piezoresistive pressure transducers, and a Schlieren system. A total of 80

channels of transient recorders with a 500 kHz sampling rate were recorded by an acquisition system.

Condition	Gas	T_0	P_0	Mach	ρ_∞	U_∞	P_∞	T_∞	Unit Re
		[K]	[bar]	[-]	[kg/m^3]	[m/s]	[Pa]	[K]	[-]
low Re	N_2	1740	550	13.9	0.0108	1880	140	44	6
med Re	N_2	1640	1100	14.3	0.0196	1820	225	39	13.2
high Re	N_2	1745	1470	14.8	0.0206	1880	235	39	17.5

Table 1: Reference conditions for the Longshot facility

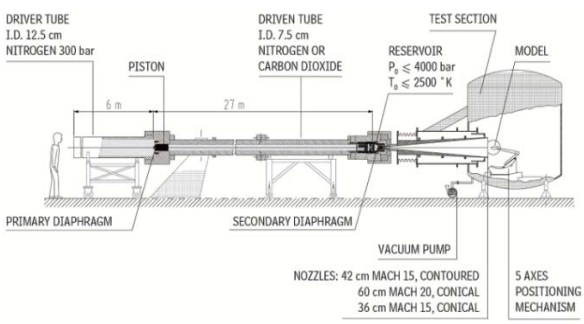

Figure 1: Sketch of the Longshot Facility

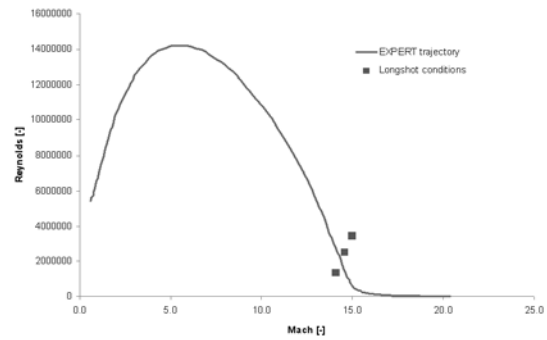

Figure 2: Longshot conditions on the Expert trajectory

B. Model and Roughness Configuration

The EXPERT wind-tunnel test model is a 228.7mm long blunt nose vehicle. It corresponds to a 14.7% scaled version of the real EXPERT vehicle. The model is shown in Figure 3 with part of its instrumentation. It is manufactured in Aluminium. The model is equipped with 21 thermocouples placed along the cone side of the model and along the flap side of the model. 11 Pressure sensors are located on the flap side of the model.

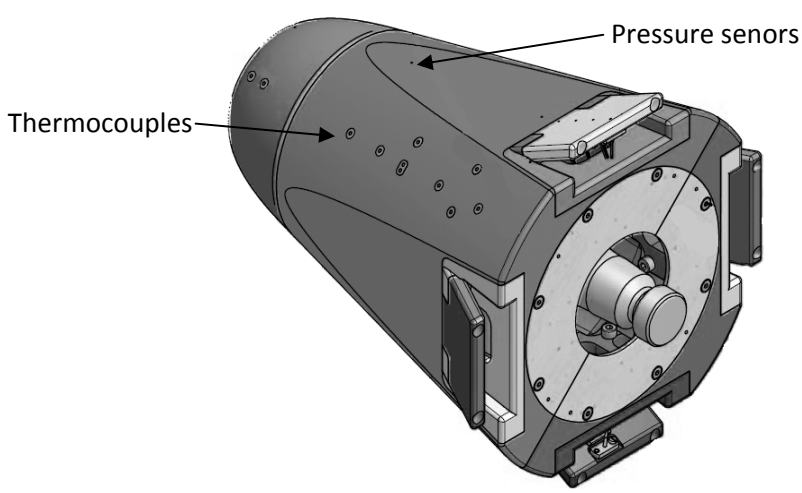

Figure 3: Model geometry and instrumentation for Longshot experiments

The distributed roughness on the nose of the vehicle cannot be geometrically scaled with the vehicle size. Rather, there is a parameter representing the height of the roughness within the boundary layer thickness which has to be respected. The aim of this study is not to evaluate whether the distributed roughness appearing in flight will trigger transition or not but is to determine the critical height triggering transition. CFD has been used along with empirical correlations to predict the critical size triggering transition. On this basis, sand grains, whose calibrated size is in the vicinity of the critical height predicted, is stuck onto the model using paint or varnish. Different heights are tested with the following ranges: [0.15-0.2mm], [0.2-0.3mm] and [0.21-0.42mm]. Examples of models equipped with such distributed roughness are shown in Figure 4.

Experiments conducted were also aiming to study the influence of the distributed roughness density parameter. Models equipped with the same size of sand grains in the range [0.15 - 0.2mm] but with different distributed roughness densities are shown in Figure 5.

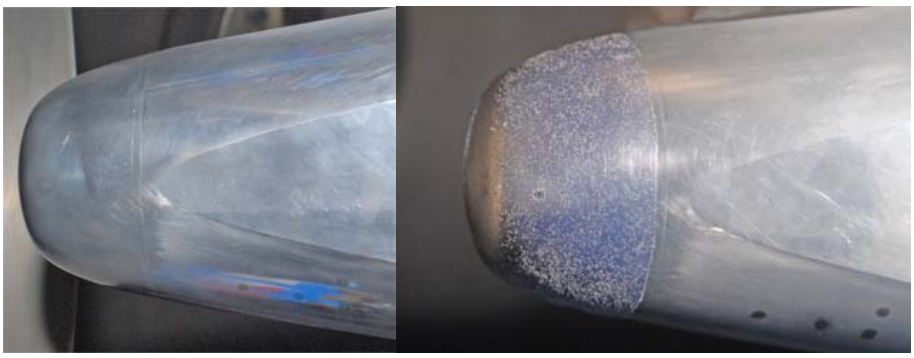

Figure 4: EXPERT model. a) Smooth model, b) h=0.15 - 0.2mm

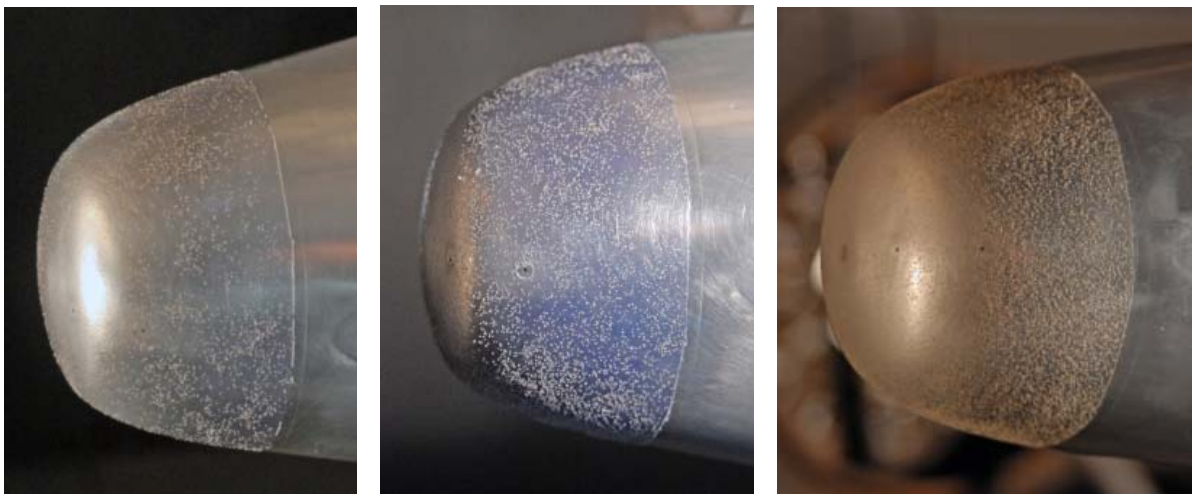

low density medium density high density

Figure 5: EXPERT model equipped with roughness [0.15 - 0.2mm], low, medium, high density

C. Thermocouples Measurements Technique

Flush mounted coaxial thermocouples are used to measure the transient surface temperature along the EXPERT model. As the wall temperature is of direct interest the probe material haves the same thermal properties as the surrounding wall to ensure a one dimensional heat flux into the probe. Two assumptions are used to compute the heat flux from the surface temperature measured with coaxial thermocouples:

- The first one is that the measurements are dominated by one-dimensional heat conduction into the probe. Therefore, only the face of the probe should be exposed to the flow. The EXPERT model used is equipped with an insert with the same thermal properties in which the gauges are mounted which reduces radial heat fluxes. The thermal properties of the thermocouples are obtained by an individual calibration provided by the manufacturer.
- The second assumption is that the probe acts as a semi-infinite body, i.e. the heat flux entering the thermocouple does not influence the temperature at its rear end.

If both assumptions are fulfilled the heat flux entering the surface can be computed using the following equation deduced from one-dimensional heat conduction theory [1]:

$$\dot{Q}(t) = \frac{\sqrt{\rho c k}}{\sqrt{\pi}} \left[\frac{T(t)}{\sqrt{(t)}} + \frac{1}{2} \int_0^t \frac{T(t) - T(\tau)}{(t-\tau)^{3/2}} \, d\tau \right]$$

This mathematical model assumes the medium into which heat is conducted has infinite thickness. It requires the measurement of the time variation of the surface temperature and assumes a constant back surface temperature at the second boundary condition. Equation above can be discretized in the following way in order to use the measured temperature data.

$$\dot{Q}(t_n) = \frac{2\sqrt{\rho c k}}{\sqrt{\pi}} \left[\sum_{i=1}^{n} \frac{T(t_i) - T(t_{i-1})}{(t_n - t_i)^{1/2} + (t_n - t_{i-1})^{1/2}} \right]$$

This equation is valid assuming t_0=0 with the temperature set to $T(t_0) = 0$, i.e. the above temperatures used represent temperature differences measured with the probe during the test with respect to the initial temperature.

In order to investigate the laminar-to-turbulent boundary layer transition of the fluid on the EXPERT model, a dimensionless heat flux (Stanton number) is introduced. It is the ratio between heat transferred to the wall and heat convected through the boundary layer. Assuming a perfect gas and a unit recovery factor, the Stanton number is given by:

$$St_M = \frac{\dot{q}_w}{\rho_\infty U_\infty c_P \left(T_W - T_0\right)}$$

D. Pressure Measurements Technique

The model tested is equipped with pressure transducers (Kulite XCS-093) from which pressure coefficients can be deduced knowing free-stream conditions.

III. Experimental Results

A. Effect of distributed roughness location

The purpose of the first investigation is to define which part of the nose plays a role in the transition. Experiments are performed in different configurations:

- Distributed roughness everywhere on the nose,
- Distributed roughness only in the subsonic region of the nose,
- Distributed roughness only in the supersonic region of the nose.

Figure 6 presents the evolution of the Stanton number along EXPERT on the flap side for these experiments. Dotted lines correspond to laminar and turbulent Stanton level obtained from CFD. Additional curves are for experiments where each symbol corresponds to one thermocouple.

The Stanton level close to the nosetip and in the region where there is distributed roughness (till 59mm from nosetip) has to be considered carefully due to the presence of distributed roughness. The curve representing the Stanton number over the smooth model corresponds to a laminar flow on the body and a transitional one over the flap. The experiment with distributed roughness in the subsonic part of the nose shows a similar evolution except on the flap where the Stanton number increases which means the flow is reaching a turbulent level earlier. Regarding to the experiment with distributed roughness over the supersonic part of the nose only, the Stanton level is higher along the body but tends to decrease along the body. It may show vortex wake heating while the flow is still laminar. However, the flow over the flap is turning turbulent immediately. The last test concerns roughness everywhere on the nose. The Stanton number is higher along the body, depicting a turbulent flow, and it remains turbulent over the flap.

Comparing the Stanton level for the model with distributed roughness everywhere and the one for distributed roughness only in the supersonic part of the nose shows a very similar behaviour. That means the roughness located on the first part of the nose is not the most important to trigger transition while the roughness size is the same and the boundary layer thickness is smaller. This phenomenon has been observed in [2] and can be explained by the strong favorable pressure gradient occurring while the nose curvature becomes more important which tends to keep the flow laminar.

Regarding to the flow developing along the cone side (Figure 6), the same conclusions are drawn. Roughness everywhere on the nose or only on the supersonic part leads to a turbulent flow over the cone. Roughness located only on the nosetip maintains a laminar flow over the first part of the cone which turns transitional only over the back of the vehicle.

In order to study the worst configuration which could arise in flight, following tests have been performed with distributed roughness everywhere on the nose.

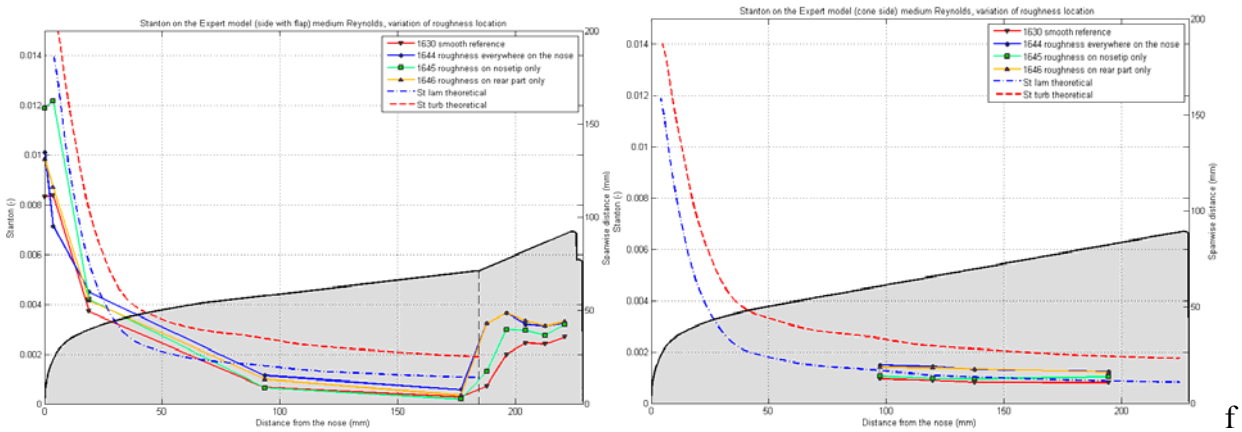

f

flap side cone side

Figure 6:Stanton number along EXPERT at medium Reynolds number, distributed roughness size in the range [0.21 - 0.42mm], variation of roughness location

B. Effect of roughness density

This campaign has been performed to assess the effects of the roughness density on the flow. Variations of Stanton number along the body are studied for different distributed roughness densities. Stanton number is compared with a fully laminar case (shot 1627, smooth model) and a fully turbulent case (shot 1644, with large roughness). Three tests (shots 1649, 1652 and 1653) have been performed with the same free-stream conditions and the same size of roughness on the model [0.15 - 0.2mm]. The only varying parameter was the distributed roughness density (1649: high density, 1652: medium density, 1653: low density).

Figure 7 shows the evolution of the Stanton number for the tests. It is shown there is an effect of the distributed roughness density on the flow. The test with the highest density shows a Stanton comparable with the fully turbulent reference case while the other ones tends toward the reference smooth case with only a transitional flow over the flap.

The flow over the cone shows a similar behavior as shown in Figure 7. The flow is turbulent for the highest density but remains laminar for lower density.

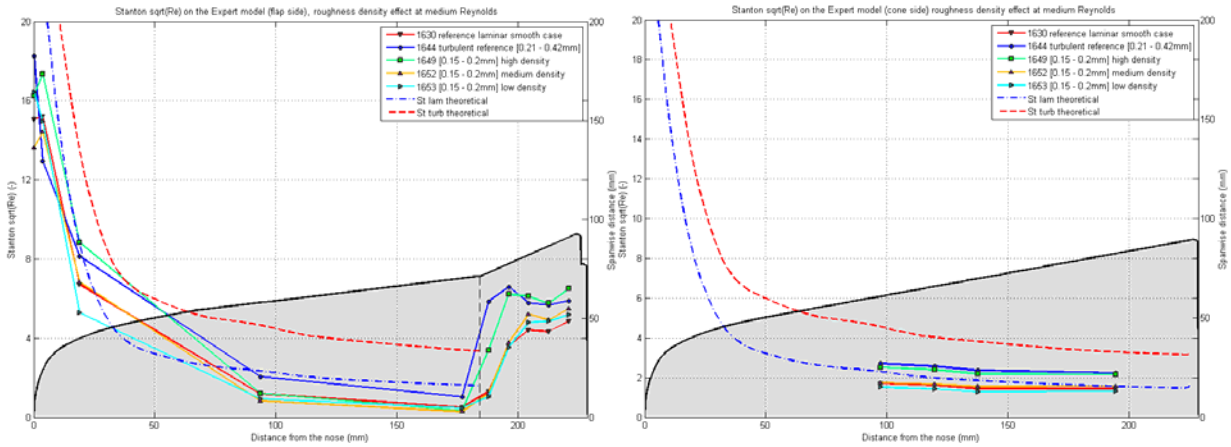

flap side cone side

Figure 7: Stanton number along EXPERT, distributed roughness size in the range [0.15 - 0.2mm], variation of distributed roughness densities

Previous section has shown an effect of distributed roughness density on the flow, but experiments have shown other phenomena described below.

Stanton number is compared for test 1652 with a fully laminar case (shot 1627, smooth model) and a fully turbulent case (shot 1644, with large roughness) at three different times: 4, 10 and 12ms from the beginning of the experiment. For each time step, the Stanton number has been extracted and Figure 8 shows the temporal evolution of the flow during the same experiment with two reference cases.

This picture shows clearly a decrease of the Stanton number with respect to time, implying an evolution of the flow from turbulent to laminar. This phenomenon has been observed for other tests (1649, 1651 and 1653) and is due to a slight decrease of the Reynolds number during the experiment (Figure 9). The evolution of the flow from turbulent to laminar has been detected on the cone side as well as shown in Figure 8.

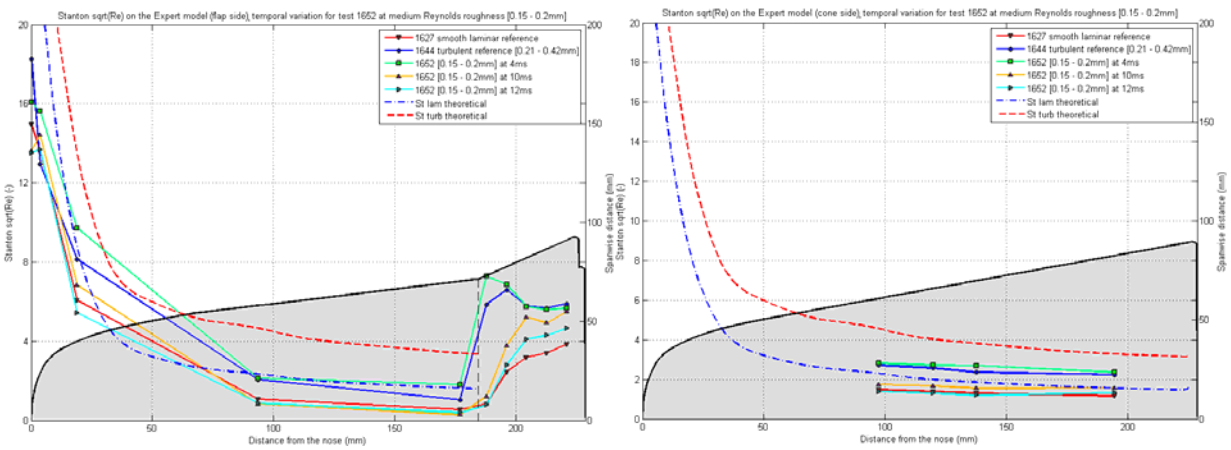

flap side cone side

Figure 8: Spatial evolution with respect to time of Stanton number along EXPERT for test 1652, distributed roughness size in the range [0.15 - 0.2mm] at medium density

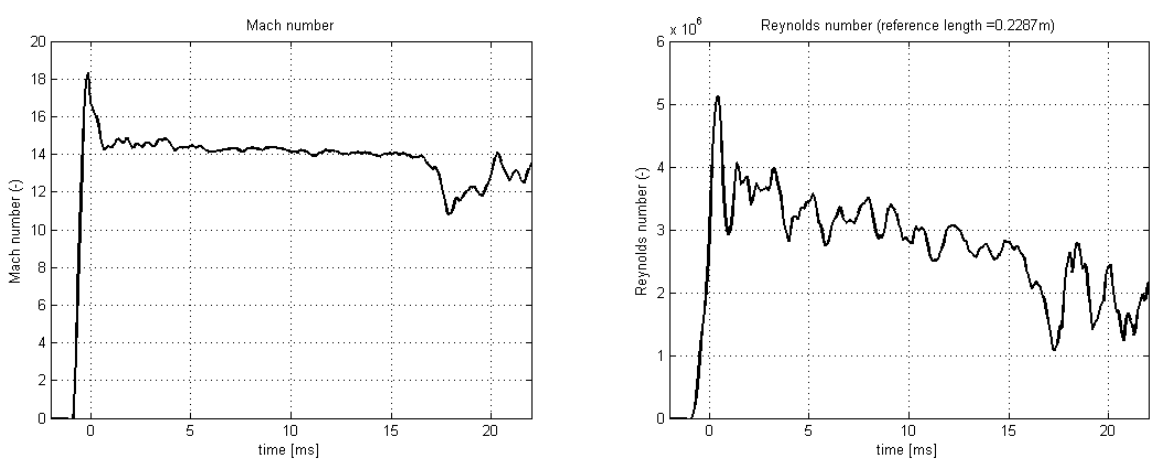

Figure 9: Temporal evolution of Mach number and Reynolds number with respect to time for shot 1652

Regarding to the pressure coefficients on the flap side a clear evolution is observed. The recirculation bubble located in front of the flap has a clear effect on the pressure coefficients. When the flow is laminar, the recirculation bubble is large and as a consequence it covers the pressure sensor before the flap until the second one on the flap. If the flow is turbulent, the recirculation bubble is much smaller and it does not cover any of the pressure sensors. Before the flap, when the flow turns turbulent, the pressure measured is lower, because the velocity of the flow at this location is now higher. On the flap, the recirculation bubble does not exist anymore and thus the flap is fully exposed to the flow inducing a higher pressure measured.

The phenomena is confirmed by Schlieren pictures extracted for the corresponding times and shown in Figure 10. Shock waves close to the flap indicate the size of the recirculation bubble.

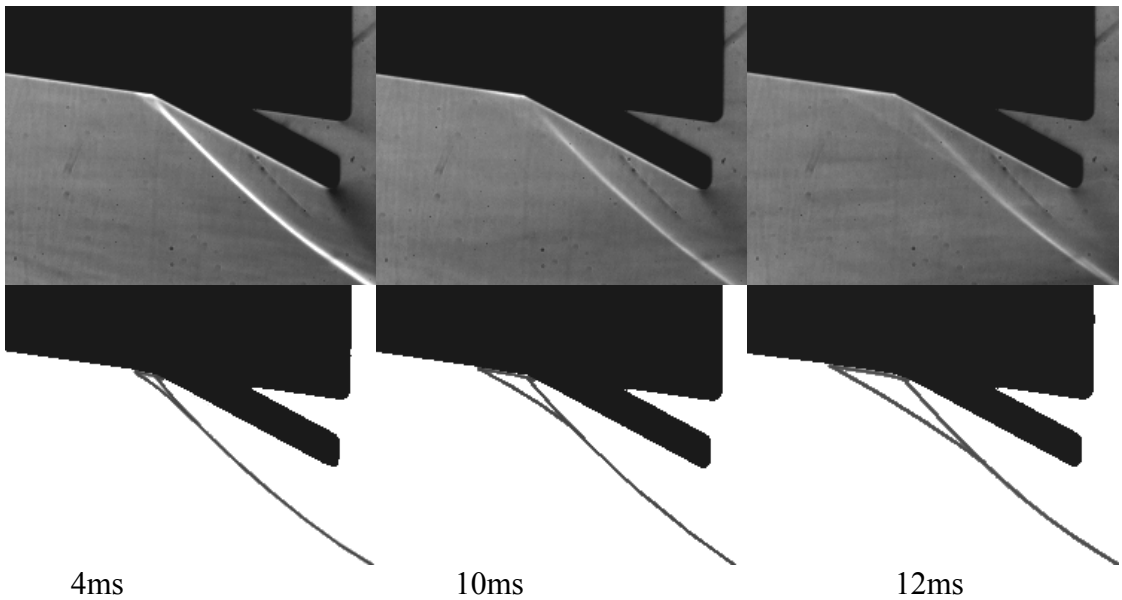

Figure 10: Schlieren of test 1652 at different time steps showing the evolution of the recirculation bubble depicting a turbulent flow and then a laminar one. Distributed roughness in the range [0.15 - 0.2mm] with medium density, at medium Reynolds number

It has been shown the flow is turning from turbulent to laminar during the experiment. However, experiments with different densities have shown the time it happens is not the same. The higher the density, the longer turbulent flow remains. Figure 11 depicts the Stanton number variation for sensor TC4 on the cone side with respect to time. The Stanton variation is plotted for each sensor during different tests in order to show how density affects the transition.

For a low distributed roughness density, the flow turns back laminar quite early. If the density is increased, the flow turns laminar but later on, once the Reynolds number has decreased further. Increasing further the distributed roughness density delayed the flow from turning laminar.

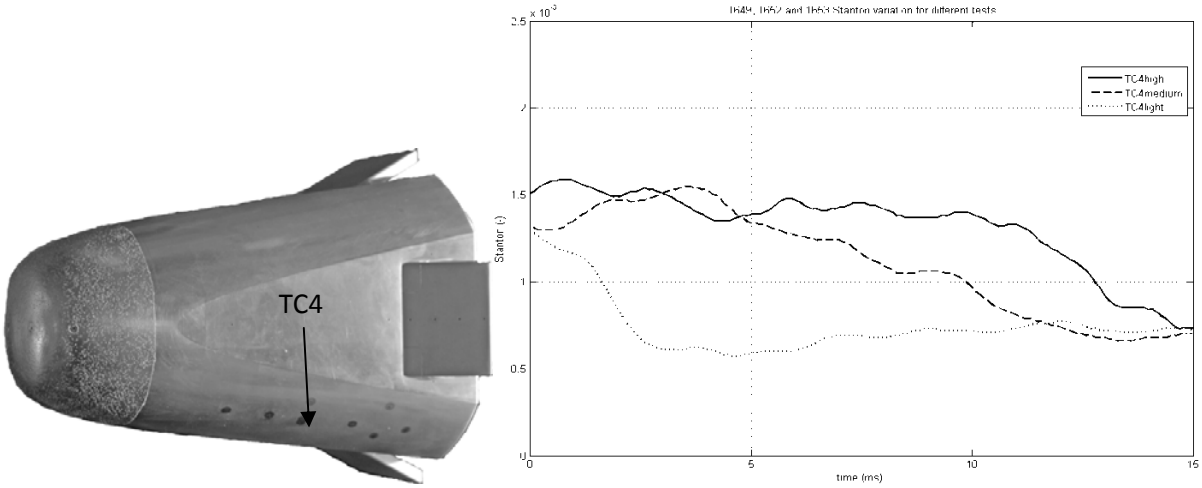

Figure 11: Temporal evolution of Stanton number along EXPERT from thermocouple TC4 for tests 1649, 1652 and 1653 (roughness size [0.15 - 0.2mm]), distributed roughness densities being high, medium and low respectively

As a conclusion, the density has an effect on the flow: the higher the density is, the sooner transition occurs. For the following experiments, the distributed roughness density used has been the medium one. The temporal effects are not reported in this study but observations have not shown large temporal effects as the ones described previously. All data reductions have been performed 10ms after the beginning of the experiment.

C. Effect of distributed roughness size

In this section, results of experiments with different sizes of distributed roughness are reported. The aim is to determine the critical height leading to transition.

Stanton numbers along the flap side are compared in Figure 12. Accurate measurements of heat transfer are not obtained in the distributed roughness region. For the reference smooth case, the flow is laminar over the flat surface and transitional over the flap. The smallest distributed roughness used ([0.15 - 0.2mm]) show a laminar flow over the flat surface which turns transitional on the flap. The Stanton level reached over the flap is greater than the one obtained for the smooth case. The increase of the size of the roughness (range [0.2 - 0.3mm]) shows a flow at the beginning of the flat surface which is not turbulent. The higher Stanton number might be due to vortex wake heating while the flow is still laminar. The flow reaches a turbulent level over the flap. Increasing further the size of the roughness (range [0.21 - 0.42mm]) shows a turbulent flow over the entire body.

The flow over the cone (Figure 12) is transitional for the smallest size of roughness ([0.2 - 0.3mm]) and will be developed in following section. For larger sizes, the flow is turbulent over the cone surface.

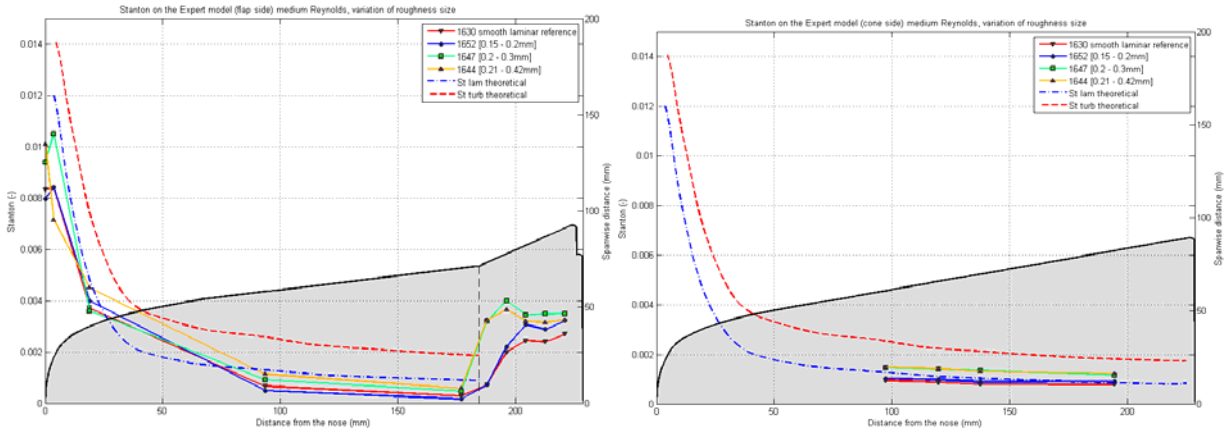

flap side cone side

Figure 12: Stanton number along EXPERT, medium Reynolds number, variation of distributed roughness size

Medium Reynolds				
Shot	Roughness	Cone side	Flat surface on flap side	Flap on flap side
1630	Smooth	Laminar	Laminar	Transitional
1652	[0.15-0.2]	Transitional	Laminar	Transitional
1647	[0.2-0.3]	Turbulent	Transitional	Turbulent
1644	[0.21-0.42]	Turbulent	Turbulent	Turbulent

Table 2: Results obtained according to sizes of roughness at medium Reynolds number

Table 2 summarizes the results obtained during experiments at medium Reynolds number. The results obtained during this campaign have then been compared to the critical heights defined by empirical correlations. Figure 13 shows this comparison. On this figure is plotted the critical height predicted by Reda and Reshotko correlations. Additionally, the distributed roughnesses tested during experiments have been added as rectangular zones. One zone corresponds to one test. The horizontal extension corresponds to the spatial extension over the model: from the nosetip to the end of the nose at 59mm. The vertical extension represents the range in which was the size of roughness. Criteria should preferably be compared along the cone as there is not the favorable pressure gradient created by the truncated surface.

From experiments, it has been seen on the cone side that roughness in the range [0.15 - 0.2] has started triggering transition and the ones in the range [0.2 - 0.3] have lead to a fully turbulent flow. Regarding to the average values, 0.175mm starts being effective and 0.25mm was fully effective. Additionally, experiments performed with the [0.15 - 0.2mm] size have shown a clear transitional flow at t=10ms over the cone. Thus any correlation predicting a critical height around 0.175mm over the nose region might be correct.

Reda criterion predicts heights which are in the vicinity of the experimental critical height of 0.175mm over the rear part of the nose. Regarding to Reshotko criterion, the largest height predicted at the nose junction is about 0.17mm.

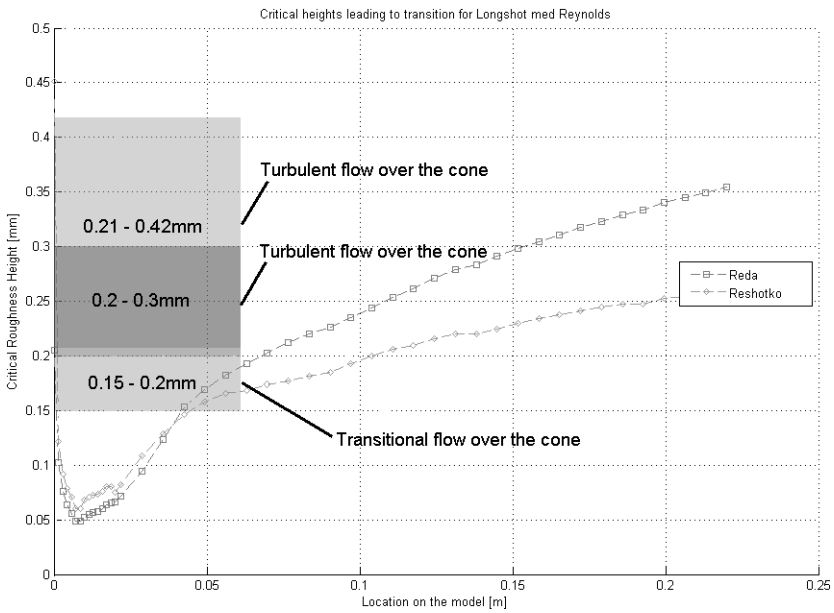

Figure 13: Estimation of critical heights leading to transition according to different criteria for Longshot facility at medium Reynolds number and comparison with experimental results

D. Extrapolation to flight conditions

The aim of this study is to determine the critical height leading to transition on the real EXPERT vehicle. This section performs the extrapolation of the results obtained in the Longshot facility to flight conditions. The flow conditions in the Longshot facility are close to the ones encountered in flight so that Mach and Reynolds similarity parameters are respected.

The extrapolation is performed for the medium Reynolds test conditions whose experiments allowed determining precisely the critical height triggering transition, that is 0.175mm (average value of the range [0.15 - 0.2mm]). The remaining unknown is the location of the distributed roughness which has effectively triggered transition. From a first approach it could be the location where the boundary layer is the thinnest, hence close to the nosetip, but this location has been shown to be less efficient. Thus, one can consider the effective location to be after the sonic line till the end of the nose. Recalling predictions given by one correlation for these locations and comparing them with the critical height seen during experiment allow defining a correction factor as being the ratio of the effective height and the predicted one. Considering then the same correlation for flight and applying the correction factors defined above leads to a correlation giving a critical height and whose uncertainty is defined by applying the correction factors.

For Reda correlation it comes:

- For Longshot facility, the critical height at the sonic line is about 0.06mm and at the end of the nose it is about 0.18.
- The critical height observed in the Longshot is 0.175mm but the precise location triggering transition is unknown.
- Correction factors are defined as $k_{observed}/k_{predicted}$ and it gets C_1=2.9 and C_3=0.97 as illustrated in Figure 14.

- Corrections factors are applied to the critical heights defined for flight (Figure 14) and it gives the critical heights with an uncertainty margin. The margin is quite wide due to the uncertainties of the location of the roughness which has been effective.

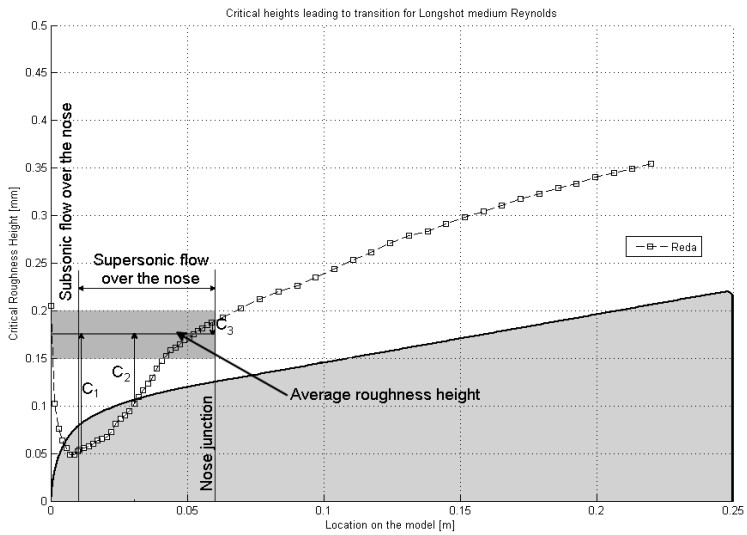

Figure 14: Determination of constants C_1, C_2 and C_3 for flight extrapolation. C_1 is considered at the sonic line, C_3 is evaluated at the nose junction and C_2 is evaluated between them in order to have an intermediate value.

Results are shown in Figure 15 for Reda and Reshotko. The thicker line corresponds to the original correlation whose uncertainty has been defined as described previously. Constants have been defined for the sonic line (x≈0.01m), for the end of the nose (x=0.059m) and for an intermediate value (x=0.03m). Grey area represents these uncertainties.

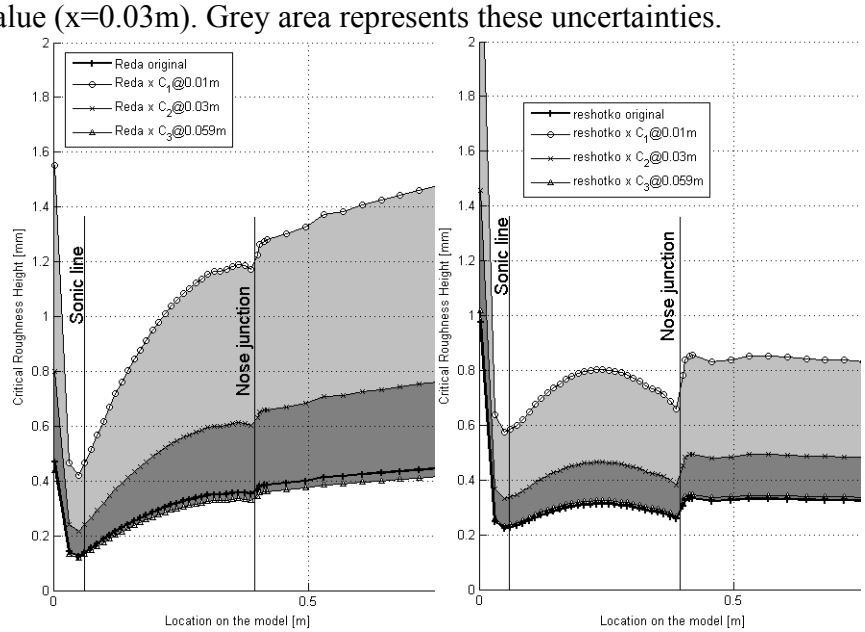

Figure 15: Critical heights triggering transition after extrapolation to real flight conditions at Mach 14 for EXPERT vehicle. The nose is extending from 0 to 0.4m.

As a conclusion, the estimated critical heights for flight are defined as:

- According to Reda: the critical height is between 0.14 and 1.19mm.
- According to Reshotko: the critical height is between 0.23 and 0.8mm.

Critical heights defined previously correspond to a vehicle flying at a zero angle of attack. Previous test campaigns at VKI in the Longshot facility have proved there was no transition over the EXPERT smooth model for an angle of attack of +/-5° for the same Reynolds number. The influence of angle of attack and distributed roughness is still unknown.

The conclusions issued in this section have been based on the most critical approach. During the flight, at Mach 14, the Reynolds number will be slightly lower than the medium Reynolds number tested in the Longshot. Thus, the vehicle will tolerate larger heights for distributed roughness. Moreover, the worst configuration with roughness everywhere on the nose has been considered. If experiments conducted in a high enthalpy facility on a sample of CSiC shows that most of distributed roughness occurs only on the nosetip, then the critical height will be much larger as roughness in this area have been shown to be less efficient to trip boundary layers. Finally, the Longshot facility is not a quiet wind-tunnel and the noise radiated from the wall of the nozzle induce earlier transition. Experiments conducted at Mach 6 in noisy and quiet flows reported in [3] have shown a large increase in the transitional Reynolds number. As a consequence, the roughness size allowed for flight will be slightly larger.

IV. Conclusion

An experimental investigation on the effect of distributed roughness induced transition for the EXPERT vehicle was conducted in the VKI Longshot Hypersonic Wind Tunnel at Mach 14 with a Reynolds number about 11.10^6/m. Boundary layer laminar-to-turbulent transition has been detected by means of the modified Stanton number evolution. Conclusions drawn have been confirmed by pressure measurements. The size of the recirculation bubble upstream the flap is also a good indication whether the flow is laminar or turbulent. Schlieren pictures, when available, are in agreement with the conclusions too.

The observations obtained from the present experiments can be summarized as follow:

- Distributed roughness located in the subsonic flow over the nose is less efficient to trigger transition than the ones in the supersonic flow. This effect can be explained by the strong favorable pressure gradient occurring on the nose when the surface curvature is important.
- The higher the density, the sooner transition occurs. Further experiments are needed in the Longshot facility to assess the unsteady phenomena observed. There is also a need to characterize precisely the density of distributed roughness for following experiments.
- The critical height for distributed roughness on the nose of the EXPERT model in the Longshot conditions is about 0.175mm.

The final aim of this study was to extrapolate the results obtained in the Longshot wind-tunnel to flight conditions. This facility runs Mach number and Reynolds number which are close to the conditions encountered during the flight conditions of the EXPERT vehicle. As a consequence there are neither Mach number effects nor Reynolds number effect to be considered. The

conservative approach used to extrapolate the critical heights to flight conditions has lead to a critical height between 0.14 and 1.19mm according to Reda and between 0.23 and 0.8mm according to Reshotko. These predictions correspond to the most critical approach considering medium Reynolds number conditions in the Longshot and distributed roughness everywhere on the nose. During flight, Reynolds number will be slightly lower so that this critical height will be slightly larger. Furthermore, it is unlikely distributed roughness will occur everywhere on the nose of the vehicle. If distributed roughness is shown to appear only on the nosetip, the critical height for distributed roughness on the nose can be substantially larger without triggering transition as this location has been shown to be less efficient.
The large uncertainties of the flight extrapolation cannot be easily reduced as reducing the extension of distributed roughness on the nose of the vehicle would change the parameters characterizing the distributed roughness.

V. References

[1] G. Simeonides - *The VKI hypersonic wind tunnels and associated measurements techniques*, Technical Memorandum 46 VKI, November 1990.

[2] A. H. Boudreau - *Artificially Induced Boundary-Layer Transition on Blunt-Slender Cones at Hypersonic speeds*, Journal of Spacecraft, Vol. 16 n°4, July-August 1979.

[3] M. P. Borg, S. P. Schneider, T. J. Julianoz - *Effect of Freestream Noise on Roughness-Induced Transition for the X-51A Forebody*, AIAA paper 2008-0592, 2008.